J|A|C|S
ARTICLES
Published on Web 06/22/2002

Molecular Packing and Morphology of Oligo(*m*-phenylene ethynylene) Foldamers

Christian Kübel,[†,‡] Matthew J. Mio,[§,⊥] Jeffrey S. Moore,[§] and David C. Martin*[,†]

Contribution from the Departments of Materials Science and Engineering, Biomedical Engineering, and the Macromolecular Science and Engineering Center, The University of Michigan, 2022 H. H. Dow Building, 2300 Hayward Street, Ann Arbor, Michigan 48105-2136, and Roger Adams Laboratory, Departments of Chemistry and Materials Science & Engineering, The Beckman Institute for Advanced Science and Technology, University of Illinois at Urbana−Champaign, Urbana, Illinois 61801.

Received March 19, 2002

Abstract: Understanding and controlling solid-state morphologies and molecular conformations is the key to optimizing the properties of materials. As an example for the influence of small chemical changes on solid-state structures, we studied oligo(*m*-phenylene ethynylene) foldamers, where the introduction of an *endo*-methyl group induces a transition from an extended all-transoid to a helical all-cisoid conformation. The resulting structural changes were analyzed by X-ray diffraction (XRD), polarized optical microscopy (POM), and low-dose high-resolution electron microscopy (LD-HREM) over several length scales from the molecular to the mesoscopic level. The strong tendency of the *endo*-methyl oligomer **1** to form stable compact helices in solution resulted in round droplets with an ordered hexagonal columnar (Col_{ho}) liquid crystalline structure, where shrinkage during the crystallization resulted in the formation of a banded texture. On the other hand, the *endo*-hydrogen oligomer **2** exhibited a very different morphology; its extended linear shape was maintained during crystallization and resulted in an extended lamellar structure, which was determined by a compromise between crystalline packing and minimization of the surface area. Another pronounced difference between both molecular structures was the ability of the extended lamellar "crystals" to bend, whereas the helices form either straight or disordered domains. In addition, both materials exhibit strong surface effects, which extend considerably inside the droplet and induce uniform bending of the supramolecular structures.

Introduction

The realization of specific solid-state morphologies with well-defined molecular conformations is key to optimizing the properties of materials. As such, the tuning of molecular conformations and intermolecular solid-state packing has become a major objective of modern materials research. By tailoring chemical structure and processing conditions, materials with new and interesting properties can be generated. A prominent example is supramolecular crystal engineering,[1−3] where small variations in molecular structure are used to modify large-scale solid-state packing and affect the properties of the bulk material. Systematic studies on discrete oligomers based on rigid, but torsionally flexible backbones have made it possible to investigate the correlation between chemical structure, three-dimensional solid-state structure, and properties of materials. For example, advances in the synthesis of poly(*p*-phenylene ethynylene)s[4] and corresponding oligomer systems have allowed a detailed characterization of the influence of side chain substituents on solid-state molecular packing.[5,6] It has been shown that these oligomeric systems exhibit lamellar morphologies, where the length of the side chains determines the spacing between oligomer backbones. Similarly, the lamellar solid-state organization of *p*-phenylene vinylenes has been studied.[7] In contrast to these para-connected aromatic compounds, *o*- and *m*-phenylenes and *o*-phenylene ethynylenes show different solid-state packing patterns: these systems have the ability to adopt helical molecular conformations.[8−10]

Nonbiological oligomers that exhibit (fold into) compact, ordered conformations in solution and in the solid state due to

* Corresponding author. E-mail: milty@umich.edu.
† The University of Michigan.
‡ Current address: FEI Company, Achsteweg Noord 5, P.O. Box 80066, 5600 KA Eindhoven, The Netherlands. E-mail: christian.kuebel@nl.feico.com.
§ University of Illinois at Urbana-Champaign.
⊥ Current address: Department of Chemistry, Macalester College, 1600 Grand Avenue, St. Paul, MN 55015. E-mail: miom@macalester.edu.

(1) Mio, M. J.; Moore, J. S. *MRS Bull.* **2000**, *25*, 36−41.
(2) Hill, D. J.; Mio, M. J.; Prince, R. B.; Hughes, T. S.; Moore, J. S. *Chem. Rev.* **2001**, *101*, 3893−4011.
(3) Moulton, B.; Zaworotko, M. J. *Chem. Rev.* **2001**, *101*, 1629−1658.
(4) Kloppenburg, L.; Song, D.; Bunz, U. H. F. *J. Am. Chem. Soc.* **1998**, *120*, 7973−7974.
(5) Bunz, U. H. F.; Enkelmann, V.; Kloppenburg, L.; Jones, D.; Shimizu, K. D.; Cladidge, J. B.; zur Loye, H.-C.; Lieser, G. *Chem. Mater.* **1999**, *11*, 1416−1424.
(6) Kloppenburg, L.; Jones, D.; Claridge, J. B.; zur Loye, H.-C.; Bunz, U. H. F. *Macromolecules* **1999**, *32*, 4460−4463.
(7) Van Hutten, P. F.; Wildemann, J.; Meetsma, A.; Hadziioannou, G. J. *J. Am. Chem. Soc.* **1999**, *121*, 5910−5918.
(8) Blake, A. J.; Cooke, P. A.; Doyle, K. J.; Gair, S.; Simpkins, N. S. *Tetrahedron Lett.* **1998**, *39*, 9093−9096.
(9) Williams, D. J.; Colquhoun, H. M.; O'Mahoney, C. A. *J. Chem. Soc., Chem. Commun.* **1994**, *14*, 1643−1644.
(10) Grubbs, R. H.; Kratz, D. *Chem. Ber.* **1993**, *126*, 149−157.

noncovalent (supramolecular) interactions are known as foldamers.[1,2] Oligo(*m*-phenylene ethynylene)s, which exhibit a fairly diverse conformational spectrum, are an example of this class of molecule. In the solid state, all-cisoid helical structures and all-transoid extended conformations are observed depending on chain length, solvent, and preparation method, thus offering an excellent opportunity to study the effect of chemical structure on molecular conformation and solid-state packing.

Oligomer series **1** and **2** (where $n \geq 10$ repeat units) are two examples that demonstrate the conformational diversity of *m*-phenylene ethynylene foldamers as previously characterized with use of absorption spectroscopy (UV−vis,[11] fluorescence,[12] circular dichroism[13−15]), microcalorimetry,[16] and mass spectrometry.[16] The molecular conformation in solution was attributed to collective nonatom specific and nondirectional interactions known as solvophobic forces: in a "good" solvent[17] such as chloroform, both the phenylacetylene backbone and triglyme ester side chains are well-solvated. Use of a more polar, "poor" solvent such as acetonitrile causes collapse as the side chains are better solvated than the backbone. By doubling back upon itself and adopting a helical conformation, the backbone can reduce its solvent-accessible surface area. These phenomena were observed as a cooperative, sigmoidal, two-state transition when oligomers **1** and **2** were titrated in mixtures of chloroform and acetonitrile and analyzed by UV or fluorescence spectroscopy.

The oligomeric foldamers were also shown to adopt distinct conformations in the solid state, depending on substitution pattern, oligomer length, and processing method (Figure 1). The examined oligomer series **1** and **2** exhibited two extreme solid-state packing motifs. In oligomer series **2**, a fully extended, all-transoid conformation was observed leading to packing in discrete lamellae.[18] For oligomer series **1**, which exhibits a greater solution-phase folding stability due to its more hydrophobic helix interior, an all-cisoid hexagonally packed helical structure was observed.[19]

To develop a more advanced understanding of molecular packing and its influence on the morphology of these oligomers, a representative example of the *endo*-hydrogen and *endo*-methyl (i.e., facing the center of the helix) oligomer series (octadecamer, $n = 18$) was analyzed by selected area electron diffraction (SAED) and low-dose high-resolution electron microscopy (LD-HREM) as described in detail below.

Experimental Procedures

Polarized Optical Microscopy. Syntheses of oligomers **1** and **2** have been reported previously.[12,19] The liquid crystalline behavior of oligomers **1** and **2** was investigated with use of a diffusion couple.[20] Approximately 0.8 wt % solutions of **1** and **2** in methylene chloride were prepared. Three to four drops of these solutions were placed between a glass slide and cover slip and observed under crossed polarizers in transmitted light as the solvent evaporated. Gradual solvent evaporation from the edges of the sandwiched samples created a concentration gradient, allowing for the examination of the phase behavior at varying concentrations.

TEM Sample Preparation. Samples suitable for TEM analysis were prepared by spreading three droplets of 0.2 wt % solutions of the oligomers in methylene chloride on 25×75 mm^2 carbon-coated mica plates. The mica plates were kept in a Petri dish with methylene chloride atmosphere to slow evaporation of the solvent. The films were dried in 24−48 h, floated off on deionized water, and picked up with 400 mesh copper grids.

TEM Operation. A JEOL 4000EX operated at 400 kV (theoretical point-to-point resolution 0.17 nm) was used for the electron microscopic analysis. Bright-field images were taken with a 30 μm objective lens aperture. In some cases, the primary beam of the defocused diffraction pattern was used instead to improve the image contrast.

Selected area electron diffraction (SAED) patterns were calibrated with respect to gold as well as several organic polymers analyzed in our laboratories.[21,22] The electron beam stability of the sample was determined from the fading of the diffraction pattern by using the screen current meter without further calibration. For the methyl-substituted oligomer **1**, different end-point doses were observed for the meridional and equatorial reflections. The *hk*0 reflections faded after $J_e = 0.03$ C/cm^2, whereas the (001) reflections were slightly more stable with $J_e = 0.09$ C/cm^2. For the unsubstituted oligomer **2**, the end-point dose for the (001) reflection was determined to be $J_e \approx 0.05$ C/cm^2.

HREM images of the oligomers were obtained under low-dose conditions.[23] The HREM images were taken at a magnification of 20000× or 30000× with an exposure time of 1.0−1.4 s and a beam current of 10 pA/cm^2, resulting in a total dose of less than 10^{-2} C/cm^2. LD-HREM images of the methyl-substituted oligomer **1** were taken at a defocus of $\Delta f = -200$ to -1000 nm. The optimum focus conditions for unsubstituted oligomer **2** with lattice spacings of $d = 9.7$ nm[18] were calculated according to $\Delta f = -d^2/2\lambda$.[20] For an acceleration voltage of 400 kV corresponding to a wavelength of 1.643 pm, this resulted in optimum defocus conditions of $\Delta f = -28600$ nm.

Digital Image Analysis. HREM images of oligomer **1** were digitized for further analysis by scanning the negative with a LeafScan 45 at a resolution of 5080 dpi. HREM images of the oligomer **2** were digitized by scanning 3 times enlarged prints with a HP Deskscan 3c at 300 dpi.

Results

The sample preparation of oligo(*m*-phenylene ethynylene)s **1** and **2** was done by slow evaporation from a thin methylene chloride film to resemble the preparation of the previously published X-ray diffraction experiments.[19] For both samples, this led to the formation of thin round droplets with a diameter of a few microns (Figure 2). Despite the similar macroscopic structure, the morphology and crystal structure were changed drastically by substituting the *endo*-hydrogen in oligomer **2** for a methyl group in octadecamer **1**.

Structure and Morphology of the Methyl-Substituted Octadecamer 1. Selected area electron diffraction (SAED) of droplets of oligomer **1** exhibited well-defined diffraction patterns corresponding to the [100] (inset Figure 2) and [1$\bar{1}$0] zones of the hexagonal structure reported previously[19] (Table 1). The chain-length independent, hexagonal unit cell was explained by

(11) Nelson, J. C.; Saven, J. G.; Moore, J. S.; Wolynes, P. G. *Science* **1997**, *277*, 1793−1796.
(12) Prince, R. B.; Saven, J. G.; Wolynes, P. G.; Moore, J. S. *J. Am. Chem. Soc.* **1999**, *121*, 3114−3121.
(13) Gin, M. S.; Yokozawa, T.; Prince, R. B.; Moore, J. S. *J. Am. Chem. Soc.* **1999**, *121*, 2643−2644.
(14) Gin, M. S.; Moore, J. S. *Org. Lett.* **2000**, *2*, 135−138.
(15) Prince, R. B.; Moore, J. S.; Brunsveld, L.; Meijer, E. W. *Chem.-Eur. J.* **2001**, *7*, 4150−4154.
(16) Prince, R. B.; Okada, T.; Moore, J. S. *Angew. Chem., Int. Ed.* **1999**, *38*, 233−236.
(17) Flory, P. J. *Principles of Polymer Chemistry*; University Press: Ithaca, NY, 1953.
(18) Prest, P.-J.; Prince, R. B.; Moore, J. S. *J. Am. Chem. Soc.* **1999**, *121*, 5933−5939.
(19) Mio, M. J.; Prince, R. B.; Kuebel, C.; Martin, D. C.; Moore, J. S. *J. Am. Chem. Soc.* **2000**, *122*, 6134.
(20) Gonzalez-Ronda, L.; Martin, D. C.; Nanos, J. I.; Politis, J. K.; Curtis, M. D. *Macromolecules* **1999**, *32*, (14), 4558.
(21) Kübel, C.; Martin, D. C. *Philos. Mag. A* **2001**, *81* (7), 1651.
(22) Kübel, C.; Lawrence, D.; Martin, D. C. *Macromolecules* **2001**, *34* (26), 9053.
(23) Martin, D. C.; Thomas, E. L. *Polymer* **1995**, *36*, 1743.

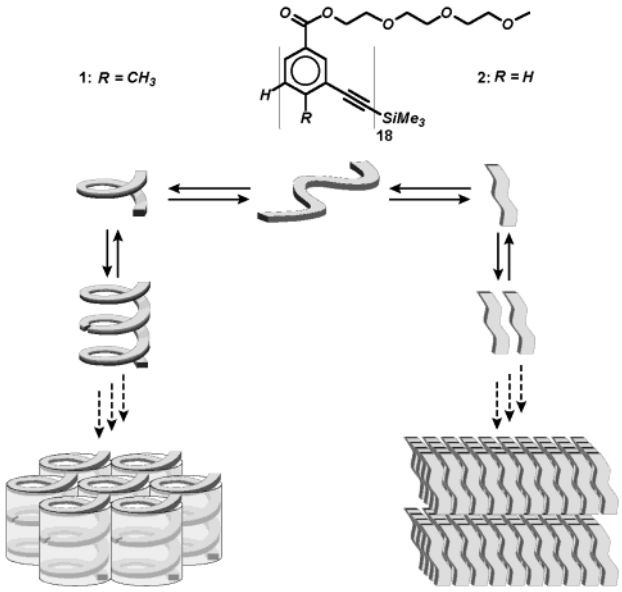

Figure 1. Schematic diagram illustrating chemical structure and packing behavior of helical (all-cisoid) and ribbon-shaped (all-transoid) *m*-phenylene ethynylene oligomers.

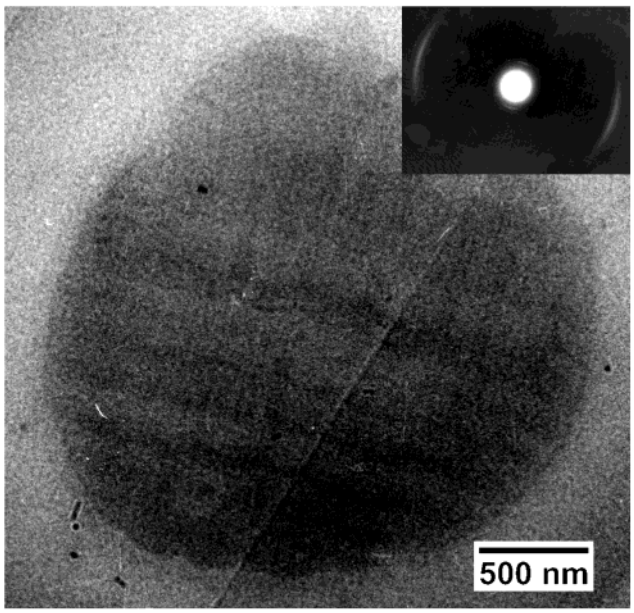

Figure 2. Defocused diffraction pattern of a droplet of the methyl-substituted octadecamer **1** crystallized by slow evaporation from dilute solution. The undulating lines correspond to shrinkage-induced changes of the helix orientation. The inset shows the electron diffraction pattern of the droplet exhibiting the (200) and (001) reflections; the (100) reflection is not visible in this figure due to inelastic scattering.

a slightly distorted 6_1 helical structure analogous to the conformation in solution.[19] The crystallographic density was determined to be 1.04 g/cm^3, which is typical for substituted aromatic materials. In this model, the (100)/(200) reflections (in the [100] zone) and the (110) reflection (in the [1$\bar{1}$0] zone) correspond to two different projections of hexagonally packed helices. The (001) reflection represents the repeat distance along the helix axis.

The diffraction pattern of a single droplet corresponded to a mono-domain with the helices oriented parallel to the carbon support film. The streaking of the diffraction patterns indicated a misorientation of the helices within this plane of about 45°.

Table 1. Comparison of Lattice Spacings Observed by X-ray Powder Diffraction for Bulk Samples and by Electron Microscopic Methods for Thin Films Showing Good Agreement

		X-ray [nm][18,19]	TEM [nm]
oligomer **1**	*hk*0	2.62 (100)	2.67 (100: HREM, SAED)
		1.51 (110)	1.56 (110: HREM, SAED)
		1.31 (200)	1.33 (200: HREM, SAED)
	*hk*1	0.36 (001)	0.36 (001: SAED)
oligomer **2**	small angle	9.76 (100)	10.0 (100: HREM)
		4.81 (200)	
		1.97 (010)	
		1.02	
	wide angle	0.77	0.75 (SAED)
		0.58	0.58 (SAED)
		0.45	0.44 (SAED)
		0.36	0.36 (SAED)
			0.224 (SAED)
			0.179 (SAED)
			0.119 (SAED)

Bright-field images of droplets of octadecamer **1** revealed weak undulating lines that were visible across the droplet (Figure 2). The undulating lines were still observed at doses higher than the end-point dose, thus indicating that they were not due to diffraction contrast, but corresponded to thickness variations within the droplet. Comparison of the orientation of the undulating lines with the diffraction pattern showed that the lines coincided with the orientation of the helix axes. Furthermore, the undulations fit to the orientation variation determined from the diffraction pattern. This suggests that the droplets were formed from helices initially extending the entire distance across the droplet.

A more detailed understanding of the morphology was obtained by low-dose high-resolution electron microscopy of the oligomer droplets. High-resolution images (Figure 3) were taken at a magnification of 30000× at a dose of about 10^{-2} C/cm^2, well below the end-point dose of oligomer **1** (see Experimental Section). In agreement with the electron diffraction observations, we obtained high-resolution images of the 2.66 (100) and 1.33 nm (200) lattice spacings corresponding to the [010] zone and 1.56 nm (110) lattice fringes in the [1$\bar{1}$0] zone. Independent of the crystallographic orientation, all droplets exhibited the same structural features. The droplets showed bands of (*hk*0) lattice fringes, which were visible across the whole droplet over a distance of several microns (Figure 3). The lattice fringes coincide with the molecular helix axes and have a length of 30−400 nm corresponding to about 80−1100 helix repeats. Between neighboring bands, the orientation of the lattice fringes changed periodically by about 45° (Figure 3b). This change in orientation was in agreement with the undulations observed in the bright-field images and is presumably related to shrinkage during evaporation of the solvent. A disordered area, where no lattice fringes were visible in the high-resolution images, mediated the change in orientation. However, the continuous features in the bright-field image (Figure 2) and the periodicity of the undulations suggested that the disorder was introduced during the shrinking process. A different behavior was observed in the vicinity of the droplet edge, where continuously bent lattice fringes could be seen (Figure 3c). This bending was only visible where it coincided with the external curvature of the droplet surface (Figure 3a). This suggested that surface effects are necessary to induce uniform lattice bending, whereas otherwise a linear arrangement of the oligomer helix is favored.

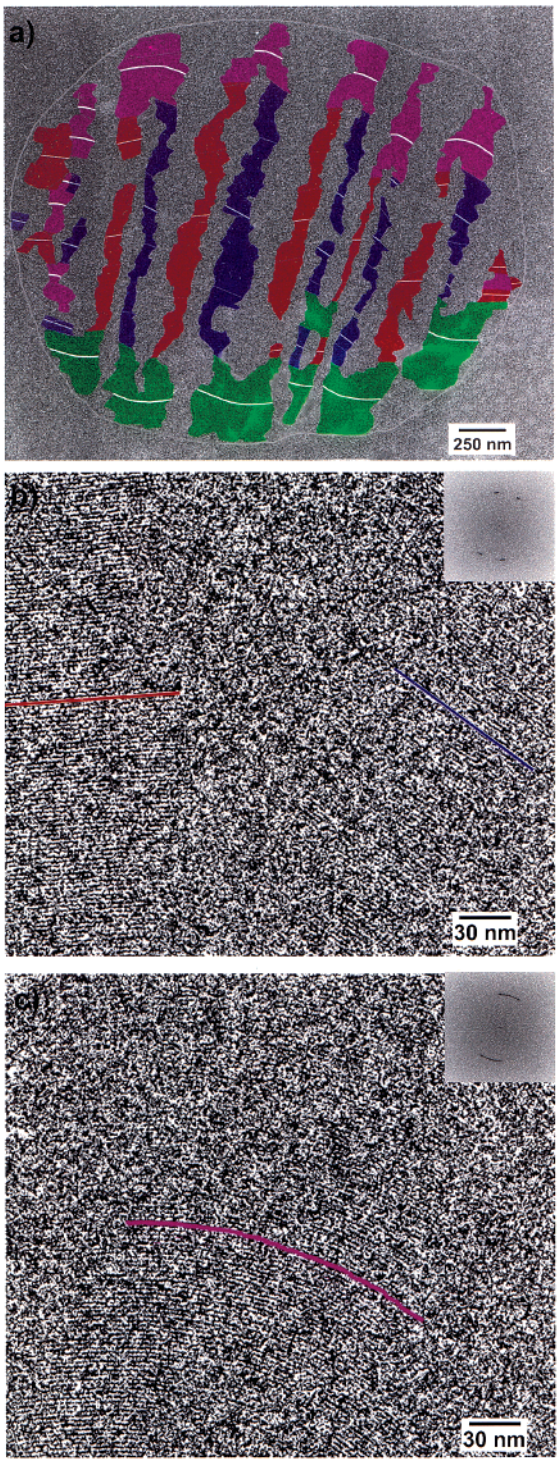

Figure 3. (a) High-resolution overview image of a droplet of oligomer **1**. The droplet exhibits domains with straight lattice fringes in the center, whereas bent lattice fringes are visible close to the surface. The color-coding depicts the areas with different kinds of lattice fringes: blue - straight down; red - straight up; green - bend upward; and purple - bend downward. (b) Enlarged area of panel a exhibiting domains with straight lattice fringes, mediated by a disordered area. The lattice fringes represent the axis of the oligomer helices. The inset shows the corresponding fast Fourier transformation of the image with two well-defined reflections. (c) Enlarged area of panel a exhibiting a domain with bent lattice fringes, corresponding to bent helices of oligomer **1**. The inset shows the corresponding fast Fourier transformation exhibiting a streaking reflection.

Structure and Morphology of the Unsubstituted Octadecamer 2. TEM analysis of droplets of the unsubstituted oligo-

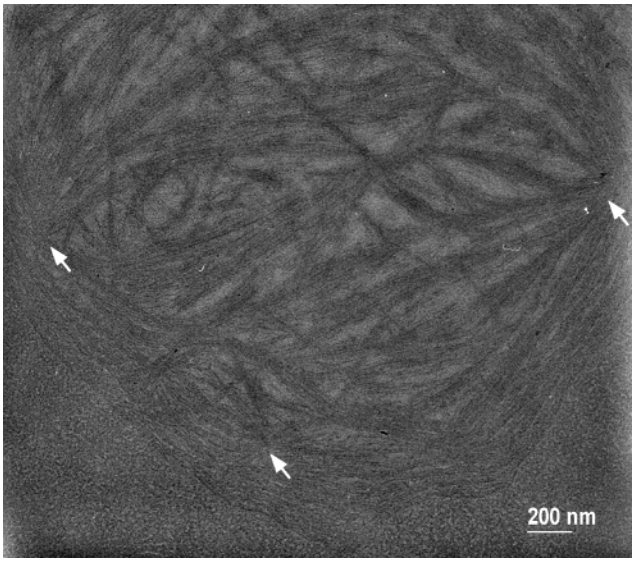

Figure 4. High-resolution electron micrograph obtained at a dose of 5×10^{-3} C/cm^2. The lattice fringes correspond to the 10 nm long spacing of the linear extended oligomer **2**. The thin crystallites are bent and form starlike intersections (white arrows).

(*m*-phenylene ethynylene) **2** showed a distinctively different microstructure compared to the methyl-substituted oligomer **1**. SAED of droplets of oligomer **2** exhibited Bragg-rings with the major reflection corresponding to 0.36 nm as well as several weak reflections, in agreement with the wide-angle X-ray experiments published previously[18] (Table 1). Small-angle reflections of 9.7, 4.85, or 1.95 nm corresponding to the size of the extended oligomer **2** were not detected due to the intensity of inelastic electron scattering at the corresponding small angles. The uniform radial intensity of the Bragg-rings showed that the oligomers did not exhibit a preferential molecular orientation within the plane of the droplet.

Even though the 9.7 nm lattice spacing visible by small-angle X-ray diffraction could not be detected by electron diffraction, we used LD-HREM at a dose of 5×10^{-3} C/cm^2 to image the corresponding lattice spacings directly at a defocus of $\Delta f = -28600$ nm. The resulting high-resolution images exhibited droplets consisting of thin long crystallites with lattice spacings of about 10 nm (Figure 4). However, the image contrast was low, since it was only due to the small electron potential difference of the end groups compared to the large oligomer. Taking high-resolution images at a slightly higher dose of 10^{-2} C/cm^2 resulted in images with much higher contrast (Figure 5), before beam damage blurred images at even higher electron doses. The lattice spacings observed at the intermediate electron dose were slightly smaller (9.3 nm), but otherwise the structural features were the same as in the low-dose images. The change in contrast was due to electron beam-induced damaging of the sample; presumably reductive cleavage of the end-groups gave rise to a higher electron potential difference. This would also explain the slightly smaller lattice spacings at intermediate doses.

Both low- and medium-dose images were analyzed to get information about the droplet microstructure. The high-resolution images of oligomer **2** exhibited droplets with an almost liquid-crystalline-like morphology. The extended oligomer chains formed long, thin, and bent "crystallites" (typically about 1000×50 nm^2) with the oligomers oriented nominally parallel to the carbon film. Within each crystallite, the oligomers

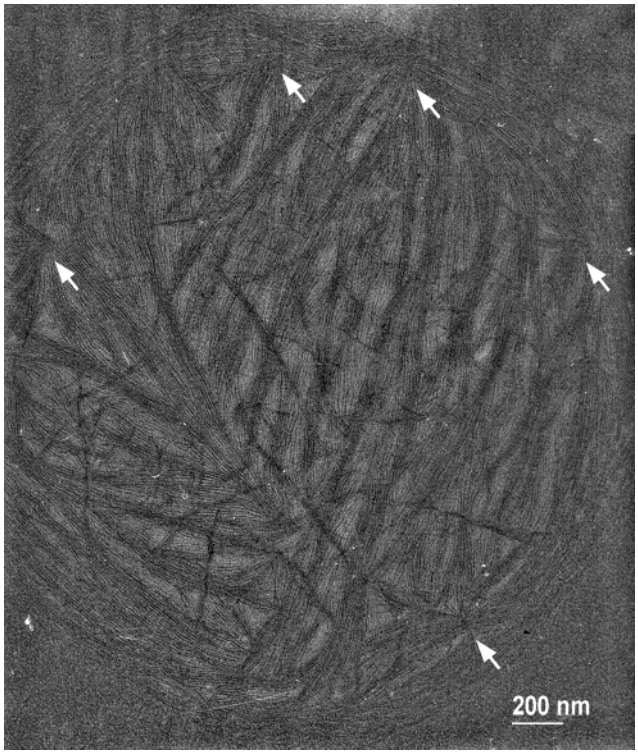

Figure 5. High-resolution electron micrograph obtained at a dose of 10^{-2} C/cm^2. Beam damage results in an improved image contrast, while the structural features are maintained. The lattice fringes correspond to the long spacing of the linear extended oligomer **2**. The thin crystallites are bent and form starlike intersections (noted with white arrows).

themselves were oriented perpendicular to the long axis. Close to the droplet edge, the crystallites were strongly bent to maintain an orientation parallel to the curved surface. Further away from the droplet edge, the crystallites were only slightly bent and randomly oriented. They exhibited a characteristic defect structure consisting of starlike crystal intersects (Figures 4 and 5).

Discussion

SAED and HREM of the *m*-phenylene ethynylene oligomers **1** and **2** showed that slow crystallization from a thin methylene chloride film resulted in a similar crystal structure as observed previously by X-ray diffraction for the bulk materials[18,19] (Table 1). The TEM and previous X-ray diffraction results both suggest that the all-cisoid (oligomer **1**) and the all-transoid (oligomer **2**) molecular conformations in solution[18,19] were maintained during crystallization, thus resulting in a helical molecular solid-state conformation for the methyl-substituted octadecamer **1** and an extended linear conformation for the unsubstituted oligomer **2** (Figure 1).

Precipitation of the helical oligomer **1** resulted in the formation of droplets with a hexagonally closed packed structure, exhibiting ordered domains of several microns in length, which were merely limited by the droplet size. Only in a single case did we ever see two different crystallographic zones coexisting in the same droplet. A similar tendency for the formation of large ordered domains by self-organization has been observed for other helical oligomers such as helicene derivatives, which crystallized with a fibrous morphology.[24,25]

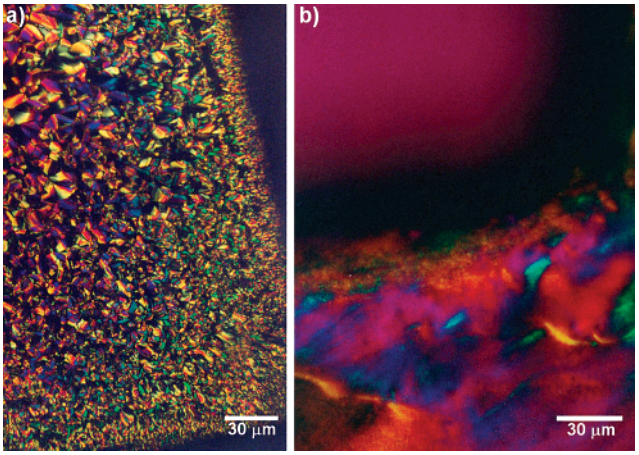

Figure 6. Polarized optical micrographs exhibiting a liquid crystalline texture for oligomers **1** and **2** in a diffusion couple. (a) Oligomer 1 shows the characteristic "fan" texture of a columnar liquid crystalline material. (b) Oligomer 2 exhibits a weak Schlieren-like texture.

The helices formed by foldamer **1** were well-defined with a measured $\pi-\pi$ stacking distance of 0.36 nm along the helix axis. Neither X-ray nor electron diffraction indicated a correlation between neighboring helices, suggesting an ordered hexagonal columnar liquid crystalline structure (Col_{ho}) with 2D + 1D order in agreement with the liquid crystalline texture observed in polarized optical microscopy (Figure 6a). However, careful inspection of the electron-diffraction pattern (inset Figure 2) showed that the (100)/(200) and (001) reflections formed an angle of about 85° with respect to each other. This indicated that the helices were distorted and grew slightly inclined with respect to the hexagonal zone, probably as a result of steric interactions between the methyl substituents in the center of the helix.

The continuous undulating lines in the TEM bright-field images (Figure 2) indicated that the oligomer helices were bent and continued throughout the whole droplet. The more detailed view obtained by high-resolution microscopy (Figure 3) showed that the apparent bending was actually due to two different linear domains which were oriented at an angle of 45° with respect to each other. This morphology resembled the structure of the "banded texture" observed in liquid crystalline polymers (LCPs) on a larger length scale.[26−29] The banded texture with feature sizes on the order of 1−20 μm was observed upon solidification[30−32] and after cessation of flow in LCPs.[26−29] After shear alignment of LCPs, bands with undulating molecular orientation were observed as a relaxation effect. It has been argued that the band formation could provide a route for stress relaxation,[26,29] e.g. for stored elastic energy[33,34] or to release dislocation loops that were stretched during flow.[35]

In the case of the oligomer droplets, the formation of the banded morphology is presumably also related to stress, which arises during shrinkage upon evaporation of the solvent. Loss of solvent during crystallization reduces the helix diameter

(24) Lovinger, A. J.; Nuckolls, C.; Katz, T. *J. Am. Chem. Soc.* **1998**, *120*, 264−268.
(25) Philips, K. E. S.; Katz, T. J.; Jockush, S.; Lovinger, A. J.; Turrow, N. J. *J. Am. Chem. Soc.* **1998**, *120*, 9541−9544.
(26) Ernst, B.; Navard, P. *Macromolecules* **1989**, *22*, 1419.
(27) Viney, C.; Donald, A. M.; Windle, A. H. *J. Mater. Sci.* **1983**, *18*, 1136.
(28) Viney, C.; Putnam, W. L. *Polymer* **1995**, *36*, 1731.
(29) Vermant, J.; Moldanaers, P.; Mewis, J *J. Rheol.* **1994**, *38*, 1571.
(30) Chen, S.; Du, C.; Jin, Y.; Qian, R.; Zhou, Q. *Mol. Cryst. Liq. Cryst.* **1990**, *188*, 197.
(31) Hoff, M.; Keller, A.; Odell, J. A.; Percec, V. *Polymer* **1993**, *34*, 1800.
(32) Song, W.; Chen, S.; Jin, Y.; Qian, R. *Liq. Cryst.* **1995**, *19*, 549.

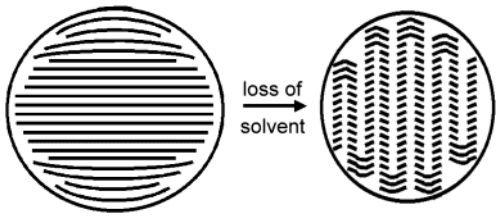

Figure 7. Schematic representation of the shrinkage-induced transition leading to the banded texture observed in the dry droplets of oligomer **1**.

thereby introducing strain perpendicular to the helices. By tilting the helices, the strain is reduced without crack formation and transferred in the direction of the helix axis, which is expected to be the direction of low viscosity in discotic liquid crystals (Figure 7). However, tilting the whole sample in one direction would require a large global reorientation. In contrast, the undulating tilt observed only requires a local reorientation, thus minimizing the overall molecular movement.

To our knowledge, the existence of disordered domains mediating the change in orientation has not been discussed for sheared liquid crystalline polymers. In the case of oligomer **1**, the disordered domains are probably related to the helices consisting of oligomers with a high end-group density thus facilitating breakage. However, the stacked helices do not necessarily break upon bending. Close to the edge of the droplet where the surface is parallel to the expected curvature mediating between two neighboring domains, the helices were continuously bent (Figure 3a,c). This indicates that the dry helices are not flexible enough to bend whereas bending due to surface effects can be achieved in the solvated state.

The small difference in the molecular structure and conformation of octadecamer **2** resulted in pronounced differences in morphology. The extended linear conformation allows for strong $\pi-\pi$-interactions between phenyl rings in neighboring molecules leading to large crystal dimensions in this direction. On the other hand, the combination of the high end-group density of these relatively short oligomers and the weak intermolecular forces between the end-groups is presumably responsible for the poor molecular packing in the direction of the backbone, which might explain the short crystal diameter corresponding to about 5 molecules. X-ray diffraction of the bulk material seemed to indicate a high degree of order, but the material was also described as a viscoelastic wax, which fits to the texture observed under crossed polarizers (Figure 6b).[18] The HREM images fit to this observation, exhibiting a structure between a crystalline and liquid crystalline material. Short- and medium-range order is visible, but long-range order is only present in one direction. The thin crystallites form a network resembling a liquid crystalline structure exhibiting a high density of starlike intersects.

The "crystals" also seem to be flexible and exhibit strong bending. Some bending is observed in the center of the droplet, but especially in the vicinity of the droplet edge, the bending is very pronounced. This surface layer has a thickness of about 200−300 nm and the crystallites are always oriented parallel to the droplet surface. Surface-induced bending of lattice planes in molecular crystals has been observed in thin droplets of diacetylenes.[36] The defect-mediated mechanisms of curvature in crystalline polymers have been recently reviewed.[37] This surface structure is distinctly different from the structure of the helical oligomers **1**, where a bimodal orientation is observed, which also exhibits domains with the helices oriented at a high angle to the surface.

Conclusions

Oligomer series **1** and **2** are chemically very similar only differing in an *endo*-methyl substitutent. Nevertheless, they exhibit distinctly different molecular conformations in solution as well as in the solid state. Using the octadecamer of each series as a representative example, we obtained further evidence supporting that oligomer **1** formed a helical molecular structure in the solid state whereas oligomer **2** crystallized with an extended lamellar conformation. The different molecular conformations were responsible for significantly different morphologies of both compounds. The strong tendency of compound **1** to form stable compact helices in solution resulted in a hexagonal discotic liquid crystalline solid-state structure with a characteristic banded texture, which is presumably formed due to relaxation upon shrinkage during evaporation of solvent. In contrast, the morphology of the droplets of oligomer **2** seemed to be determined by a compromise between crystalline packing and minimization of the surface area. Another difference between both molecular conformations is the ability of the extended lamellar "crystals" to bend, whereas the helices form either straight or disordered domains away from the surface.

Overall, these two compounds clearly demonstrate the ability to control the molecular conformation and thereby the supramolecular solid-state structure by small changes of the chemical structure. In addition, both materials also exhibited strong surface effects, which extended considerably inside the droplet. This enabled us to study the interplay between bulk packing, surface alignment, and local molecular bending.

Acknowledgment. C.K. thanks the Alexander von Humboldt foundation and the German Ministerium für Bildund und Forschung for a postdoctoral scholarship. D.C.M. thanks the National Science foundation and the Alexander von Humboldt foundation for financial support. This material was also supported by the U.S. Department of Energy, Division of Materials Sciences under Award No. DEFG02-96ER45439, through the Frederick Seitz Materials Research Laboratory at the University of Illinois at Urbana−Champaign.

JA0204022

(33) Burghardt, W. R.; Fuller, G. G. *J. Rheol.* **1990**, *34*, 959.
(34) Lee, S.; Meyer, R. B. Elastic and viscous properties of lyotropic polymer nematics. In *Liquid Crystallinity in Polymers*; Ciferri, A., Ed.; VCH: New York, 1991; p 343.
(35) Marrucci, P.; Maffetone, P. L. LCP defect dynamics in shear flows. In *Proceedings of the Third International Workshop on LCPs*; Carfanaga, C., Ed.; Pergamon: New York, 1994.
(36) Wilson, P. M.; Martin, D. C. Dislocation Mediated Lattice Bending in 1,6-Di (*N*-Carbazolyl)-2,4 Hexadiyne (DCHD) Polydiacetylene Droplets. *J. Mater. Res.* **1992**, *7(11)*, 3150−3158.
(37) Kübel, C. L.; Gonzalez, R.; Drummy, L. F.; Martin, D. C. Defect-mediated Curvature and Twisting in Polymer Crystals. *J. Phys. Org. Chem.* **2000**, *13(12)*, 816−829.